

RBM15-mediating MDR1 mRNA m⁶A methylation regulated by the TGF- β signaling pathway in paclitaxel-resistant ovarian cancer

JIA YUAN^{1,2}, WENCAI GUAN¹, XIN LI^{1,2}, FANCHEN WANG^{1,2}, HUIQIANG LIU^{1,2} and GUOXIONG XU¹⁻³

¹Research Center for Clinical Medicine, Jinshan Hospital, Fudan University, Shanghai 201508;

²Department of Oncology, Shanghai Medical College, Fudan University, Shanghai 200032;

³Center for Tumor Diagnosis and Therapy, Jinshan Hospital, Fudan University, Shanghai 201508, P.R. China

Received April 5, 2023; Accepted July 19, 2023

DOI: 10.3892/ijo.2023.5560

Abstract. Ovarian cancer (OC) lacks effective biomarkers for diagnosis at an early stage and often develops chemoresistance after the initial treatment at an advanced stage. RNA-binding motif protein 15 (RBM15) is an RNA m⁶A methylation mediator that serves an oncogenic role in some cancers. However, the function and molecular mechanisms of RBM15 in ovarian tumorigenesis and chemoresistance remain to be elucidated. The present study identified the overexpression of RBM15 in OC tissues and paclitaxel (PTX)-resistant cells using reverse transcription-quantitative (q)PCR, western blotting and immunohistochemistry. Clinical data analyses showed that high expression of RBM15 was associated with poor prognosis in patients with OC. Overexpression of RBM15 led to an increase in cell viability and colony formation and a decrease in cell sensitivity to PTX and apoptosis, whereas the knockdown of RBM15 resulted in the inhibition of cell viability and

colony formation *in vitro* and tumor formation *in vivo* and increased cell apoptosis and sensitivity to PTX in a time- and dose-dependent manner. Furthermore, RBM15 knockdown reduced the spheroid formation of PTX-resistant OC cells. Silencing of RBM15 decreased multidrug resistance 1 (MDR1) mRNA m⁶A methylation detected by the methylated RNA immunoprecipitation-qPCR assay and downregulated the expression of a chemo-drug efflux pump MDR1 at the mRNA and protein levels. Finally, RBM15 expression was suppressed by the activation of the TGF- β signaling pathway. Thus, the findings revealed a TGF- β /RBM15/MDR1 regulatory mechanism. Targeting RBM15 may provide a novel therapeutic strategy for the treatment of PTX-resistant OC.

Introduction

Ovarian cancer (OC) is the second leading cause of gynecological cancer-related deaths in women worldwide (1). The current therapy for patients with advanced-stage OC is cytoreductive surgery combined with platinum-taxane chemotherapy (2). Most patients with OC are sensitive to initial chemotherapy, but some eventually develop chemoresistance and relapse (3). Therefore, the treatment of recurrent OC remains a key challenge.

The occurrence and formation of chemoresistance consist of a diverse range of determinants, including inherent genetic mutations in tumors, cancer stem cells (CSCs), activation of intrinsic signaling pathways and pharmacological factors (4). The multidrug resistance 1 (*MDR1*) gene, also termed ATP-binding cassette sub-family B member 1 (*ABCB1*), encodes a protein called P-glycoprotein (P-gp) and is aberrantly expressed in most cancers, which promotes the efflux of intracellular chemotherapy drugs and facilitates the development of chemoresistance (5). A number of types of cancer, including OC, contain CSCs, which are considered cells that are resistant to chemotherapy (6). Our previous study showed that the paclitaxel (PTX)-resistant cells act as stem cell-like cells that expressed stem cell biomarkers such as CD44 (7). CD44 is a cell surface glycoprotein that correlates with chemoresistance in OC (8,9) and can upregulate MDR1 in doxorubicin-resistant cells (10).

Correspondence to: Professor Guoxiong Xu, Research Center for Clinical Medicine, Jinshan Hospital, Fudan University, 1508 Longhang Road, Shanghai 201508, P.R. China
E-mail: guoxiong.xu@fudan.edu.cn

Abbreviations: CCC, clear cell carcinoma; CSCs, cancer stem cells; DFS, disease-free survival; EC, endometrioid carcinoma; HGSC, high-grade serous carcinoma; IP, immunoprecipitation; LGSC, low-grade serous carcinoma; IC₅₀, the half-maximal inhibitory concentration; IHC, immunohistochemistry; MDR1, multidrug resistance 1; MeRIP, methylated RNA immunoprecipitation; OC, ovarian cancer; OS, overall survival; PBS, phosphate-buffered saline; PFA, paraformaldehyde; PFS, progression-free survival; PTX, paclitaxel; RT-qPCR, reverse transcription-quantitative PCR; RBM15, RNA binding motif protein 15; RT, reverse transcription; SBE, Smad binding element; shRNA, short hairpin RNA; siRNA, small interfering RNA; TSS, transcriptional start site

Key words: chemoresistance, N⁶-methyladenosine, RNA binding, Smad, signal transduction

N^6 -methyladenosine (m^6A) modification is the richest and reversible mRNA modification dynamically regulated by methyltransferase complexes (also called ‘Writer’), demethylases (‘Eraser’) and m^6A -binding proteins (‘Reader’) (11). RNA methylation is a post-transcriptional regulation process that affects the transcription, splicing, translation and stability of mRNAs. A previous study indicated that m^6A modification is closely correlated with tumorigenesis, cell proliferation, metastasis and chemoresistance in malignant tumors (12). RNA-binding motif protein 15 (RBM15; also termed OTT1) is a member of the split-end (SPEN) protein family, comprising three N-terminal RNA recognition motifs, also known as the RNA binding domain or ribonucleoprotein domain (13). RBM15 is an essential regulator of RNA m^6A methylation modification and a critical component of the methyltransferase complex that binds and recruits the Wilms' tumor 1-associating protein-methyltransferase like 3 complex to specific RNA sites (14). A number of studies have shown that RBM15 facilitates tumor progression as an m^6A mediator in several types of cancer (15-18). Evidence has emerged that cell signaling pathways, such as the TGF- β signaling pathway, regulate downstream gene expression through m^6A processing (19). However, the role and molecular mechanisms of RBM15 in OC and chemoresistance have not yet been completely explored.

The present study evaluated the expression, function and regulation of RBM15 in OC *in vivo* and *in vitro* and explored for the first time, to the best of the authors' knowledge, that RBM15 mediated MDR1 expression through mRNA m^6A methylation. Moreover, the association of RBM15 with PTX resistance and the prognosis of patients with OC was assessed. Finally, regulation of the RBM15/MDR1 axis by the TGF- β signaling pathway was examined.

Materials and methods

Cell lines and culture. The human immortal ovarian surface epithelial cell line IOSE-80 (originating from normal ovarian epithelium; OriGene Technologies, Inc.) and the human OC cell line OVCAR-3 (originating from ovarian adenocarcinoma derived from ascites; ATCC) were cultured in RPMI-1640 medium (Gibco; Thermo Fisher Scientific, Inc.) with 10 and 20% fetal bovine serum (FBS; Invitrogen; Thermo Fisher Scientific, Inc.), respectively. Human OC cell lines ES2 [originating from ovarian clear cell carcinoma but the genetic profile closely related to serous carcinoma (20); ATCC], A2780 (originating from ovarian endometrioid adenocarcinoma) and its PTX-resistant counterpart A2780-PTX (Nanjing KeyGen Biotech Co., Ltd.) were cultured in DMEM (Gibco; Thermo Fisher Scientific, Inc.) supplemented with 10% FBS. The human OC cell line SK-OV-3 (originating from ovarian endometrioid adenocarcinoma derived from ascites; ATCC) and its PTX-resistant counterpart SK3R-PTX [established in our laboratory] (21) were cultured in 10% FBS McCoy's 5A medium (Biological Industries). Cell line 293T (Shanghai Fuheng Biotechnology Co., Ltd.) was cultured in DMEM supplemented with 10% FBS. All the cells were cultured in a humidified incubator at 37°C and 5% CO₂. All cell lines were authenticated by short tandem repeat analysis with routine detection of pathogen-free and mycoplasma-negative.

Overexpressing plasmid and small interfering (si)RNA transfection and short hairpin (sh)RNA infection. The RBM15-overexpressing plasmid was generated by inserting a coding sequence of the RBM15 gene at positions 30-2963 (GenBank Accession no. NM_022768.5) into the multiple cloning site of the pcDNA3.1 vector (Invitrogen; Thermo Fisher Scientific, Inc.). siRNA and shRNA targeting RBM15 were synthesized by Shanghai GenePharma Co., Ltd. The sequences are listed in Supplementary Table SI. X-tremeGENE siRNA Transfection Reagent (Roche Applied Science) was used for the transfection of siRNAs and overexpressing plasmids according to the manufacturer's instructions. After the incubation of transfection mixture at room temperature for 15 min, cells were transfected with either 2 μ g/well of siRNAs or 2.5 μ g/well overexpressing plasmids in a 6-well plate for 24 h at 37°C, followed by subsequent experimentation. RBM15-shRNAs and negative control shRNA (sh-NC) were synthesized by Genewiz, Inc. and cloned into lentiviral shRNA-overexpressing plasmids (Hanbio Biotechnology Co., Ltd.). Cells were seeded in 12-well plates and were infected at 20-30% confluence by adding the lentiviral RBM15-shRNA overexpressing plasmid or the control lentiviral supernatant for 48 h at 37°C, followed by subsequent experimentation.

RNA extraction and reverse transcription-quantitative (RT-q) PCR. Total RNA was extracted when cell density reached at 90% confluence using the RNA-Quick Purification Kit (Shanghai Yishan Biotechnology Co., Ltd.; cat. no. ES-RN001). RT of RNA to complementary DNA was performed using a qPCR RT kit (Roche Diagnostics). PCR was performed using BeyoFast SYBR Green qPCR Mix (2X; High ROX; Beyotime Institute of Biotechnology). RNA extraction, cDNA synthesis, and qPCR were performed according to the manufacturer's protocols and cycling conditions were: Initial denaturation at 95°C for 1 min followed by 40 cycles of denaturation at 95°C for 10 sec and annealing/extension at 60°C for 30 sec. The threshold cycle (Cq) was determined using the 7300 real-time PCR system (version 1.4, Applied Biosystems; Thermo Fisher Scientific, Inc.). Actin was used as an internal control for gene expression. According to the obtained Cq values, the expression of target genes was quantitatively analyzed by $2^{-(\Delta\Delta Cq)}$ (22). Experiments were repeated at least three times. The PCR primer sequences are listed in Table SI.

Protein extraction and western blot analysis. The cells were lysed with sodium dodecyl sulfate lysate (Beyotime Institute of Biotechnology) containing 1% phenylmethanesulfonyl fluoride (Beyotime Institute of Biotechnology) and 1% phosphatase inhibitor. After the total protein was extracted, the protein concentration was measured using a BCA protein assay kit (Beyotime Institute of Biotechnology) by microplate spectrophotometer (Epoch, BioTek Instruments, Inc.). Protein samples (25 μ g/lane) were subjected to 10% sodium dodecyl sulfate-polyacrylamide gel electrophoresis and transferred to PVDF membranes. After the membranes were blocked with 5% non-fat milk for 1 h at room temperature, they were incubated with primary antibodies at 4°C overnight. The following antibodies were used: Anti-RBM15 antibody (1:1,000 dilution; cat. no. 10587-1-AP) and anti- β -actin (1:5,000 dilution; cat. no. 66009-1-Ig) from Proteintech Group, Inc. anti-MDR1

(1:5,000 dilution; cat. no. 13342S), anti-cyclin D1 (1:2,000 dilution; cat. no. 2978S), anti-phosphorylated (p)-Smad2 (1:1,000 dilution; cat. no. 3101S) and anti-Smad2 (1:1,000 dilution; cat. no. 3103S) from Cell Signaling Technology, Inc. The secondary antibody anti-mouse IgG (1:5,000 dilution; Proteintech Group, Inc.; cat. no. SA00001-1) or anti-rabbit IgG (1:5,000 dilution; Proteintech Group, Inc.; cat. no. SA00001-2) was then used at room temperature for 1 h. Protein bands were photographed and quantified using a chemiluminescence imaging system (Tanon-4500, software v4.1.5; Tanon Science and Technology Co., Ltd.).

Human ovarian tissue preparation and immunohistochemistry (IHC) staining. A total of nine non-tumor ovarian tissues and 18 OC tissues, including 1 clear cell carcinoma (CCC), 2 endometrioid carcinomas (EC), 11 high-grade serous carcinomas (HGSC) and four low-grade serous carcinomas (LGSC), were obtained from the Jinshan Hospital of Fudan University for the initial IHC study. None of the patients had received chemotherapy or radiotherapy before surgery. Ethics approval was approved by The Ethics Committee of Jinshan Hospital (approval no. JYLLKY-2019-01-01). For IHC analysis, 4% paraformaldehyde (PFA)-fixed paraffin-embedded tissue specimens were sectioned (4 μ m thick). After deparaffinization in xylene and rehydration in a descending alcohol series, 3% hydrogen peroxide in methanol was applied to quench the endogenous peroxidase activity. After blocking with 10% normal goat serum (Fuzhou Maixin Biotech. Co., Ltd.) for 40 min at room temperature, the sections were incubated with a primary anti-RBM15 antibody (1:150 dilution; Proteintech Group, Inc.; cat. no. 10587-1-AP) at 4°C overnight, followed by a biotinylated secondary anti-rabbit antibody (cat. no. KIT-5020; Fuzhou Maixin Biotech. Co., Ltd.) for 1 h at room temperature. After staining with a DAB kit (cat. no. DAB-1031; Fuzhou Maixin Biotech. Co., Ltd), images were captured using a light microscope (BX43; Olympus Corporation).

Tissue microarray. A tissue microarray containing 45 OC tissues paired with 45 adjacent-noncancerous tissues was obtained from Shanghai Outdo Biotech Co., Ltd. (cat. no. OVC0901). Ethical approval was obtained from the Ethics Committee of the Shanghai Outdo Biotech Company (approval no. TRLL-2020-035-01). Detailed clinical information was obtained. Histological assessment and classification were determined according to the criteria of tumor, node and metastasis classification by the American Joint Committee on Cancer (<https://www.facs.org/quality-programs/cancer-programs/american-joint-committee-on-cancer/version-9/>). The tumor stage was diagnosed based on the International Federation of Gynaecological Oncologists system (<https://www.igo.org/>). IHC was performed using a primary anti-RBM15 antibody (1:150 dilution; Proteintech Group, Inc.; cat. no. 10587-1-AP) and a biotinylated secondary anti-rabbit antibody (Fuzhou Maixin Biotech. Co., Ltd.; 50 μ l; cat. no. KIT-5020) at room temperature for 30 min. After IHC on 45 pairs of samples, six pairs were either invalid or missing during the process and the final 39 pairs of valid samples (8 EC, 16 HGSC, 14 LGSC and 1 CCC) were evaluated using a Panoramic 250 FLASH scanner (3DHISTECH Ltd.). After staining with a DAB kit (Fuzhou Maixin Biotech. Co., Ltd.), the results were assessed

blindly by two independent investigators according to the staining area and intensity. The staining index (SI) of RBM15 was calculated by the sum point of i) one of the percentage scores of immuno-positive cells: 0 (no positive cells), 1 (\leq 25%), 2 (26-50%), 3 (51-75%), 4 (>75%) and ii) one of the staining intensity score: 0 (no coloration), 1 (pale brown), 2 (brown), 3, (dark brown), as described previously (23). Finally, the SI of RBM15 was clustered into three groups: negative expression (0-2 sum points), low expression (3-5 sum points) and high expression (6-7 sum points). In addition, the overall survival (OS) and disease-free survival (DFS) time of OC patients were analyzed by Kaplan-Meier analysis using 'survival' (version 3.3.1) (<https://github.com/therneau/survival>), 'survminer' (<https://rpkgs.datanovia.com/survminer/index.html>), 'ggplot2' (version 3.3.6) (<https://github.com/tidyverse/ggplot2>) R packages.

Analyses of gene/protein expression from the public database. The data for differentially expressed genes between OC and normal ovarian samples were extracted from the Gene Expression Omnibus (GEO, <https://www.ncbi.nlm.nih.gov/geo/>) (24) and analyzed using the 'impute' (version 1.64.0) and 'limma' (version 3.46.0) (25) R packages. Protein expression data extracted from the Clinical Proteomic Tumor Analysis Consortium (CPTAC) were analyzed using the UALCAN database (<http://ualcan.path.uab.edu/index.html>) (26). RNA-seq data from various OC cell lines were downloaded from the CCLE website (<https://sites.broadinstitute.org/ccle>) and analyzed. After screening for RBM15-associated genes, Gene Ontology (GO) enrichment analysis and Kyoto Encyclopedia of Genes and Genomes (KEGG) pathway enrichment analysis were performed using 'limma' (version 3.46.0) (25), 'ggplot2' (version 3.3.6) (<https://github.com/tidyverse/ggplot2>), 'ggpubr' (version 0.6.0) (<https://rpkgs.datanovia.com/ggpubr/>), 'ggExtra' (version 0.10.0) (<https://github.com/daattali/ggExtra>), 'clusterProfiler' (version 4.8.1) (27), 'org.Hs.eg.db' (version 3.17.0) (<https://www.bioconductor.org/>), 'enrichplot' (version 1.20.0) (<https://www.bioconductor.org/>) R packages and Gene Set Enrichment Analysis (GSEA; version 4.1.0; Broad Institute, Inc.). The data on RBM15 expression associated with patient survival were analyzed using the Kaplan-Meier Plotter (<http://kmplot.com/analysis>) (28). The specific procedure was stepped as inputting the Gene symbol RBM15 first, selecting 'the Auto select best cutoff' and finally analyzing OS and PFS, respectively (retaining the default values for other parameters). Gene Expression Profiling Interactive Analysis (GEPIA), an online analytical database (<http://gepia.cancer-pku.cn/>) based on gene expression data from tumor and normal samples in The Cancer Genome Atlas (TCGA) and Genotype-Tissue Expression databases (29), was used for analyzing the correlation between RBM15 and MDR1 expression in OC.

Drug sensitivity analysis. The 'pRRophetic' (30) R package (<http://genemed.uchicago.edu/~pgeelehrer/pRRophetic/>) was used to measure the difference in the half-maximal inhibitory concentration (IC₅₀) of different drugs between the RBM15 high and the low expression group from TCGA-Ovarian Cancer.

Immunofluorescence staining. Cells were seeded in a 35 mm confocal culture dish with a 20 mm glass bottom at 10^5 cells/dish. After confluence reached 50-70%, cells were fixed with 4% PFA for 15 min and washed with phosphate-buffered saline (PBS) for 5 min. After the cells were permeabilized with 0.1% Triton X-100 in PBS for 15 min, QuickBlock Blocking Buffer for Immunol Staining (Beyotime Institute of Biotechnology) was applied for 1 h at room temperature. Cells were incubated with the primary anti-RBM15 antibody (1:200; Proteintech Group, Inc.; cat. no. 10587-1-AP) at 4°C overnight, followed by incubation with the secondary antibody (Alexa Fluor 594-conjugated goat anti-rabbit IgG; 1:500 dilution; cat. no. 8760S; Cell Signaling Technology Inc.) for 2 h at room temperature in the dark. After staining with DAPI (Beyotime Institute of Biotechnology) for 5 min, images were captured using a BioTek Cytation C10 Confocal Image Reader (Agilent Technologies, Inc.).

Cell viability, EdU and colony formation. For the cell viability assay, A2780-PTX and SK3R-PTX cells were transfected with RBM15-siRNAs and A2780 and SK-OV-3 cells were transfected with RBM15-overexpressing plasmids. A2780/A2780-PTX and SK-OV-3/SK3R-PTX cells were seeded in 96-well plates at densities of 3×10^3 and 5×10^3 cells/well, respectively. Cell viability was determined at 0, 24, 48 and 72 h by measuring absorbance at 450 nm using a CCK-8 kit (Beyotime Institute of Biotechnology) using Multiscan Spectrum (BioTek Instruments, Inc.).

For the EdU cell proliferation assay, cells were seeded in 24-well plates with 10^4 cells/well and cultured to 30-40% confluence. Cells were labeled using the BeyoClick EdU-555 kit (Beyotime Institute of Biotechnology) according to the manufacturer's instructions and images captured under a fluorescence microscope (Olympus Corporation) at x100 magnification.

For the colony formation assay, the cells were seeded in 6-well plates at a density of 1×10^3 cells/well and cultured for ~2 weeks. When the cell colonies reached the optimum confluence, 4% PFA was applied for 30 min at room temperature to fix them. A 1% crystal violet solution (MilliporeSigma) was used to stain the colonies for 30 min at room temperature. The number of cell colonies was analyzed using the ImageJ software (version 1.46r; National Institutes of Health, Bethesda, MD, USA).

Paclitaxel sensitivity assay. PTX-resistant cells were transfected with 2 μ g/well of RBM15-siRNA (si-RBM15) or negative control siRNA (si-NC) and PTX-sensitive cells were transfected with 2.5 μ g/well of RBM15-overexpressing plasmid (oe-RBM15) or negative control empty plasmid (oe-NC) in 6-well plates at the cell density of 70-80% confluence using X-tremeGENE siRNA Transfection Reagent (Roche Applied Science). After transfection at 37°C for 24 h, cells were detached and replated into 96-well plates at a density of 7×10^3 cells/well for 24 h. For dose-dependent experiments, the transfected cells were treated with different concentrations of PTX for 48 h. Cell viability was determined using a CCK-8 kit and the IC_{50} was calculated by nonlinear regression analysis using a model of 'Log(inhibitor) vs. normalized response-Variable slope' under the 'Dose-response-Inhibition'

section and presented with a 95% confidence interval (95% CI). Next, a time-course experiment was performed using a CCK-8 kit after the cells were treated with PTX at the IC_{50} concentration for 24, 48 and 72 h.

Detection of cell apoptosis by flow cytometry. Cells were seeded into the 6-well plate with 10^5 cells/well. After transfection with 2 μ g/well of RBM15-siRNA or 2.5 μ g/well of RBM15-overexpressing plasmids at 37°C for 24 h using X-tremeGENE siRNA Transfection Reagent (Roche Applied Science), the cells were treated with or without PTX (IC_{50} concentration) for 24 h when cell confluence reached ~90%. Next, the cells were digested with an EDTA-free trypsin (GENOMBIO), washed with pre-cooled PBS and resuspended in 100 μ l of 1X binding buffer, followed by the addition of 1 μ l of Annexin V-FITC and/or 2 μ l of propidium iodide according to the manufacturer's instructions (BD Biosciences). After incubation at room temperature in the dark for 15 min and the addition of 400 μ l of 1X binding buffer to each tube, apoptotic cells were detected by flow cytometry (Gallios; Beckman Coulter, Inc.). The apoptotic rate was calculated as the percentage of early + late apoptotic cells using FlowJo v10.6.2 (FlowJo LLC).

Spheroid formation of cancer stem cell-like cells. RBM15-shRNA- or NC-shRNA-infected cells were seeded in a 6-well ultra-low attachment culture plate (Corning, Inc.) at a density of 1×10^3 cells/well and cultured in serum-free DMEM/F12 cell medium (Gibco; Thermo Fisher Scientific, Inc.) supplemented with 20 ng/ml epidermal growth factor (EGF; Thermo Fisher Scientific, Inc.), 20 ng/ml basic fibroblast growth factor (bFGF; Thermo Fisher Scientific, Inc.), 4 μ g/ml heparin (MilliporeSigma) and 0.4 μ g/ml B27 (Thermo Fisher Scientific, Inc.). The grown spheroids were recorded every 2 days until day 11 and the diameter radius (r) of a microspheroid was determined by measuring two mutually perpendicular (length d1 and width d2) using the formula $r = 1/2 \times \sqrt{d1 \times d2}$.

Tumor xenograft mouse model. Animal studies were approved by the Laboratory Animal Welfare and Ethics Committee of the Shanghai Public Health Clinical Center (approval no. GWLL2020-A0270-01). A total of 15 5- to 6-week-old female BALB/c nude mice (weight 17-20 g; Shanghai Super-B&K Laboratory Animal Corp. Ltd.) received water and food *ad libitum* and were provided constant temperature (22-25°C), humidity (50-60%) and a 12-h light/dark cycle in the animal facility. A total of 5×10^6 NC-shRNA- or RBM15-shRNA-infected A2780-PTX cells in 100 μ l medium were subcutaneously injected into the right flank of mice (n=5/group). Mice without any intervention were used as blank controls (n=5). Body weight, tumor initiation and tumor progression were monitored every other day for 29 days (day of tumor formation=day 1). Tumor volume was calculated using the formula $V = ab^2/2$, where V was the volume and a and b represent the tumor length and width, respectively. On day 30, the animals were anesthetized using 20 μ l/g of 2% tribromoethanol by intraperitoneal injection and sacrificed by cervical dislocation and the tumors were excised and images captured.

Methylated RNA immunoprecipitation (MeRIP)-PCR assay. The MDR1 m⁶A methylation region was predicted using a sequence-based RNA adenosine methylation site predictor (SRAMP; <http://www.cuilab.cn/sramp>) (31) and primers were designed to amplify the high-m⁶A region. Total RNA was extracted from si-NC- and si-RBM15-transfected A2780-PTX and SK3R-PTX cells using TRIzol (Thermo Fisher Scientific, Inc.) when the cell confluence reached at 90%. Immunoprecipitation (IP) of m⁶A-containing mRNAs was performed using a Methylated RNA Immunoprecipitation Kit (Guangzhou BersinBio Biotechnology Co., Ltd.). Briefly, after concentration measurement, 100 μ g RNA was chemically fragmented and diluted in 850 μ l IP buffer plus 4 μ l RNase Inhibitor. Then, 50 μ l RNA was used for input and the remaining RNA (400 μ l each) was incubated with N⁶-methyladenosine antibody or negative immunoglobulin G (IgG) antibody supplied by the kit at 4°C for 4 h and subsequently bound with magnetic beads at 4°C for 2 h according to the manufacturer's instructions. After washing with the IP buffer, a 25:24:1 mixture of phenol, chloroform and isoamyl alcohol (MilliporeSigma) was applied to extract and purify RNA. Finally, RT-qPCR was conducted to quantify the input RNA, isolated m⁶A-containing RNA and isolated IgG control RNA. The cycling condition was the same as it in the above RT-qPCR subsection. The $2^{-\Delta\Delta Cq}$ values were calculated using a formula of $\Delta Cq = [Cq(IP) - Cq(Input) - \log 2^{DF}]$, where DF indicates the input dilution factor, to assess RNA expression from the eluate over the input samples as a percentage.

TGF- β 1 treatment. SK3R-PTX cells were seeded in a 6-well plate overnight, followed by treatment with 10 ng/ml recombinant human TGF- β 1 (R&D Systems, Inc.) at 37°C for 24 h. For the inhibition of TGF- β signaling, cells were pretreated with the TGF- β receptor kinase inhibitor SB431542 (10 μ M; MilliporeSigma) for 0.5 h and followed by TGF- β 1 (10 ng/ml) treatment for 24 h.

Dual-luciferase reporter assay. According to the scoring of the binding sites of the Smad Binding Element (SBE) predicted by JASPAR (<https://jaspar.genereg.net/>) (32), the length of the DNA sequence with the highest score was chosen for cloning. Briefly, two different lengths of RBM15 promoter with or without SBE [-1081 and -780 bp upstream from the transcription start site (TSS)] were amplified and ligated into the pGL4-Basic vector (Promega Corporation) to generate P1081 and P780 plasmids. 293T cells were cotransfected with pGL4 and the control *Renilla* luciferase vector pRL-SV40 for 24 h using Lipo8000 (Beyotime Institute of Biotechnology), followed by treatment with or without 10 ng/ml TGF- β 1 for 24 h. Luciferase activity was measured using a Dual-Luciferase Reporter Gene Assay Kit (Shanghai Yeasen Biotechnology Co., Ltd.) by Fluoroscan Ascent FL (Thermo, Thermo Fisher Scientific, Inc.) with the formula: Luciferase activity = $(F_{\text{experimental}} - F_{\text{background}}) / (R_{\text{experimental}} - R_{\text{background}})$, where F indicates luminescence value of Firefly luciferase and R indicates luminescence value of *Renilla* luciferase.

Statistical analysis. All data were analyzed using GraphPad Prism 8.0 (Dotmatics) and R version 4.1.3 (R Foundation for Statistical Computing, Vienna, Austria) (<http://www.R-project.org/>). Unpaired Student's t-test was used for two-group

comparisons. Multiple t-tests were used for multiple groups comparison. One-way ANOVA followed by the Tukey or Dunnett test and two-way ANOVA followed by the Sidak or Tukey test were used to compare continuous variables among ≥ 3 groups according to the type of experiment where indicated. For a non-parametric analysis when the sample distributions were not normally distributed, a Mann-Whitney test was used. To determine non-random associations between two categorical variables, a Fisher's exact test was used. To compare unpaired two samples, a Wilcoxon test was used. $P < 0.05$ was considered to indicate a statistically significant difference.

Results

RBM15 is overexpressed in OC cell lines and OC tissues. Compared with the normal human ovarian surface epithelial (IOSE-80) cells, RBM15 expression was higher in OC cells (OVCAR-3, ES2 and A2780) at the mRNA and protein levels, as detected by RT-qPCR and western blotting, respectively (Fig. 1A-C). High expression of RBM15 protein was also observed in OC tissues (n=18) compared with non-tumorous ovarian tissue (n=9), as detected by IHC staining (Fig. 1D and E). By analyzing public data extracted from two GEO datasets GSE14407 (12 serous papillary OC cases) (33) and GSE12470 (35 advanced serous OC cases and 8 early serous OC cases) (34), it was found that RBM15 mRNA was overexpressed in ovarian primary malignant tumor tissues compared with that in normal ovarian epithelial tissues (Fig. S1A). Furthermore, the expression level of RBM15 protein was also higher in ovarian primary malignant tumor tissues than in normal ovarian epithelial tissues when analyzing data from the CPTAC database (Fig. S1B). Tissue microarray analysis confirmed the high expression of RBM15 in ovarian malignant tumor tissues compared with adjacent non-cancerous tissues among 39 OC cases ($P < 0.001$; Fig. S1C and D). These findings indicated that RBM15 was a tissue biomarker for OC.

High expression of RBM15 is associated with poor prognosis of OC patients. Next, the present study examined the association between RBM15 expression and clinicopathological features. Based on the IHC index scores, the high expression (index score > 5) and low expression (index score ≤ 5) groups were defined. Clinical data analysis from 39 OC cases demonstrated that high expression of RBM15 was positively associated with advanced stage ($P = 0.045$), higher level of serum biomarker CA125 ($P = 0.036$) and recurrence ($P = 0.045$; Table SII). Further analysis showed that high RBM15 expression was associated with shorter OS and DFS in patients with OC (Fig. S2A and B). Further analysis of the clinical dataset using the Kaplan-Meier Plotter database (<http://kmplot.com/analysis/index.php?P=service&cancer=ovar>) confirmed that high expression of RBM15 was associated with poor prognosis in OC patients (dataset # 1555760_a_at; Fig. S2C and D). These data indicated the prognostic value of RBM15 in OC patients.

RBM15 is overexpressed in OC PTX-resistant cells and increases cell viability. By comparing PTX-resistant cells with their PTX-sensitive counterparts, it was found that RBM15

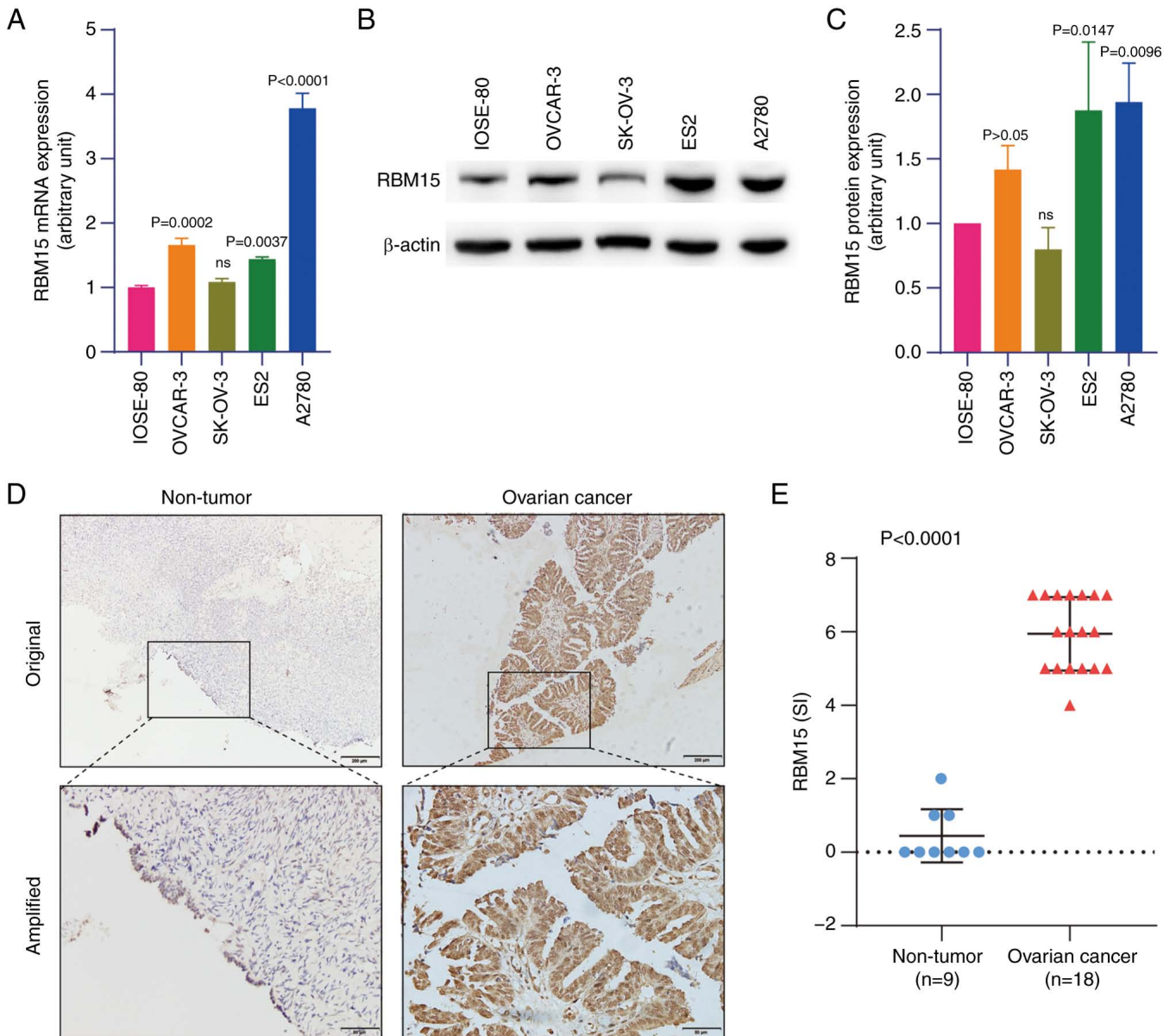


Figure 1. RBM15 expression in OC cell lines and OC tissues. (A) Detection of RBM15 mRNA expression in immortal ovarian surface epithelial cells (IOSE-80) and epithelial ovarian cancer cells (OVCAR-3, SK-OV-3, ES2 and A2780) by reverse transcription-quantitative PCR. One-way ANOVA followed by the Dunnett test was used. Data presented as mean \pm SD (n=3). (B) Detection of RBM15 protein expression in ovarian cell lines by western blot analysis. Representative images are shown. (C) Semiquantitative analysis of blots in (B). One-way ANOVA followed by the Dunnett test was used. Data presented as mean \pm SD (n=3). (D) Detection of RBM15 protein expression in non-tumorous ovarian tissue and primary ovarian cancer tissue by immunohistochemistry staining. Representative images are shown. Original magnification \times 100; Scale bar, 200 μ m. Partial magnification \times 400; Scale bar, 50 μ m; (E) Comparison of RBM15 protein expression between non-tumorous ovarian tissue (n=9) and primary ovarian cancer tissue (n=18) using the Mann-Whitney test. Data presented as mean \pm SD. ns, not significant (P>0.05). RBM15, RNA binding motif protein 15; OC, ovarian cancer; SI, staining index.

mRNA expression was higher in A2780-PTX and SK3R-PTX cells than in A2780 and SK-OV-3 cells, as detected by RT-qPCR (Fig. S3A). Western blotting showed high expression of the RBM15 protein in A2780-PTX and SK3R-PTX cells (Fig. S3B and C), as confirmed by immunofluorescence (Fig. S3D and E).

To examine the function of RBM15 in OC cells, RBM15-siRNA was synthesized and RBM15-shRNA and RBM15-overexpressing plasmids generated. A2780-PTX cells were transfected with three RBM15-siRNAs and the transfection efficacy was evaluated after the detection of the RBM15 protein by western blotting (Fig. S4A). The sequence of one RBM15-siRNA was used to generate the RBM15-shRNA

plasmid, which was cloned into the lentivirus. It was found that sh-RBM15 was more efficient in knocking down the target gene in PTX-resistant cells (Fig. S4B). The efficacy of RBM15-overexpressing plasmid was tested in PTX-sensitive cells. It was found that RBM15 mRNA and protein levels were increased in SK-OV-3 and A2780 cells, as detected by RT-qPCR and western blotting (Fig. S4C and D).

Next, the present study explored the effect of RBM15 on the proliferation of PTX-resistant and PTX-sensitive cells. Loss-of-function and gain-of-function approaches showed that cell viability was decreased after the knockdown of RBM15 by si-RBM15 and increased after the overexpression of RBM15 by oe-RBM15 in a time-course manner (Fig. 2A, C, E and G).

Moreover, the EdU assay verified that the knockdown of RBM15 decreased DNA replication, whereas overexpression of RBM15 increased DNA replication in A2780-PTX, SK3R-PTX, A2780 and SK-OV-3 cells (Fig. 2B, D, F and H). Western blotting further detected a decrease in the protein expression of cyclin D1, a cell proliferation-related marker, after the knockdown of RBM15 in PTX-resistant OC cells (Fig. S4E). These data indicated that RBM15 may regulate cell proliferation.

Knockdown of RBM15 leads to an inhibition of colony formation in vitro and tumor formation in vivo. The colony formation assays showed that the knockdown of RBM15 by RBM15-siRNA suppressed colony formation in A2780-PTX and SK3R-PTX cells (Fig. 3A and B), whereas overexpression of RBM15 by overexpressing plasmids significantly accelerated colony formation in A2780 and SK-OV-3 cells (Fig. 3C and D) compared with the negative control group. Next, stable RBM15-overexpressing A2780-PTX cells were generated and subcutaneously injected into nude mice to validate the effect of RBM15 on tumor growth *in vivo*. It was found that tumor formation was suppressed in sh-RBM15 mice (Fig. 3E). The tumor weight and volume were decreased in sh-RBM15 mice, indicating that RBM15 knockdown inhibited tumor growth (Fig. 3F and G).

Knockdown of RBM15 resensitizes PTX-resistant cells to paclitaxel. Since the level of RBM15 expression was higher in PTX-resistant OC cells than in their sensitive counterparts, whether knockdown or overexpression of RBM15 affected cell sensitization to PTX was tested. The cytotoxicity assay showed a change in PTX-resistant cell viability after knockdown or overexpression of RBM15, as evaluated by measuring the IC_{50} of PTX. RBM15 knockdown increased the sensitivity of A2780-PTX and SK3R-PTX cells, whereas RBM15 overexpression increased the resistance of A2780 and SK-OV-3 cells to PTX in a dose-dependent manner (Fig. 4A and B). The IC_{50} value decreased from 8.768 μ M (95% CI 6.377 to 12.06) to 1.457 μ M (95%CI 0.8106 to 2.619) in A2780-PTX cells and from 2.646 μ M (95%CI 0.3162 to 22.14) to 0.909 μ M (95%CI 0.08733 to 9.470) in SK3R-PTX cells after si-RBM15 transfection (Fig. 4A), whereas it increased from 0.021 μ M (95%CI 0.007197 to 0.06488) to 0.093 μ M (95%CI 0.03337 to 0.2151) in A2780 cells and from 0.038 μ M (95%CI 0.004525 to 0.3230) to 0.139 μ M (95%CI 0.01688 to 1.148) in SK-OV-3 cells after oe-RBM15 transfection (Fig. 4B). Repeated experiments showed that the average IC_{50} value significantly declined from 7.365 \pm 1.308 μ M to 1.581 \pm 0.337 μ M in A2780-PTX cells (n=3; P=0.0018) and from 2.465 \pm 0.161 μ M to 0.833 \pm 0.079 μ M in SK3R-PTX cells (n=3; P<0.0001) after si-RBM15 transfection (Fig. 4C), whereas it raised from 0.034 \pm 0.013 μ M to 0.118 \pm 0.035 μ M (n=3; P=0.0172) in A2780 cells and from 0.064 \pm 0.026 μ M to 0.148 \pm 0.039 μ M (n=3; P=0.0371) in SK-OV-3 cells after oe-RBM15 transfection (Fig. 4D). Although the sigmoidal nature of these plots in Fig. 4A and B was not ideal, the results for the IC_{50} calculations (Fig. 4C and D) were sufficient to indicate the differences in cell viability and IC_{50} between the NC and RBM15 knockdown/overexpression groups. Knockdown of RBM15 decreased the viability of A2780-PTX and SK3R-PTX cells, while overexpression of RBM15 increased

the viability of A2780 and SK-OV-3 cells in a time-dependent manner after treatment with IC_{50} dose of PTX (Fig. 4E and F). These results indicated that high expression of RBM15 was positively associated to the high IC_{50} value of PTX. Further, it was analyzed whether RBM15 expression was associated to other anti-cancer drugs in OC treatment. Using a public data source (<http://genemed.uchicago.edu/~pgeeheher/pRRophetic/>), it was found that veliparib, cyclophosphamide, elesclomol, pictilisib, lapatinib, temsirolimus and vinblastine were associated with RBM15 expression (Fig. S5A-G). These data suggested that RBM15 is an anti-cancer drug resistance-related gene. One of the reasons for chemoresistance is the reduction in cell apoptosis. Next, the effect of RBM15 on PTX-resistant cell apoptosis was examined by flow cytometry. RBM15 knockdown or overexpression alone did not affect apoptosis. However, the number of apoptotic cells was significantly increased in the si-RBM15 group of A2780-PTX and SK3R-PTX cells but decreased in the oe-RBM15 group of A2780 and SK-OV-3 cells after PTX treatment (Fig. S6A-F). These data indicated that RBM15 is a therapeutic target for PTX resistance in terms of proliferation and that RBM15-siRNA is a sensitizer of PTX in terms of apoptosis.

Knockdown of RBM15 inhibits PTX-resistant cell stemness. Next, whether RBM15 also affects cancer cell stemness in PTX-resistant cells was explored, since PTX resistance is positively correlated with stem cell characteristics (7). A2780-PTX and SK3R-PTX cells were stably infected with sh-RBM15 or sh-NC virus and these stable cells were then seeded in an ultra-low attachment culture plate. The growth of stem cell-like cells was measured by spheroid formation assays. It was found that the spheroid-forming capacity of sh-RBM15 cells was remarkably lower than that of sh-NC cells (Fig. S7A-C). These data suggested that the knockdown of RBM15 may inhibit PTX-resistant cell stemness.

Silencing of RBM15 decreases MDR1 mRNA m⁶A methylation. To further explore the specific molecular mechanism regulating resistance in OC, the correlation between RBM15 expression and MDR1 expression in OC was assessed using the GEPIA database and measured by Spearman Correlation Coefficient (Fig. 5A). The effect of RBM15 on MDR1 expression was validated by RT-qPCR and western blotting. Knockdown of RBM15 significantly inhibited MDR1 mRNA and protein expression (Fig. 5B-D). As RBM15 is a critical component of the m⁶A methyltransferase complex (14) and since RBM15 affects MDR1 expression, the SRAMP database was next applied to predict the possible distribution of m⁶A sites in MDR1 mRNA. Multiple m⁶A modification sites in MDR1 mRNA were found (Fig. 5E). Subsequently, the MeRIP-qPCR assay demonstrated that RBM15 knockdown significantly reduced the m⁶A level of MDR1 mRNA, covering 4,449 and 4,478 sites (Fig. 5F). These data suggested that RBM15 regulates MDR1 expression through m⁶A modifications.

RBM15/MDR1 expression is downregulated by activating the TGF- β /Smad2 signaling pathway. To understand the biological functions of RBM15 in OC, RNA-seq data from 47 OC cells were downloaded from CCLE (<https://sites.broadinstitute.org/ccle>) and analyzed. There were 79 genes

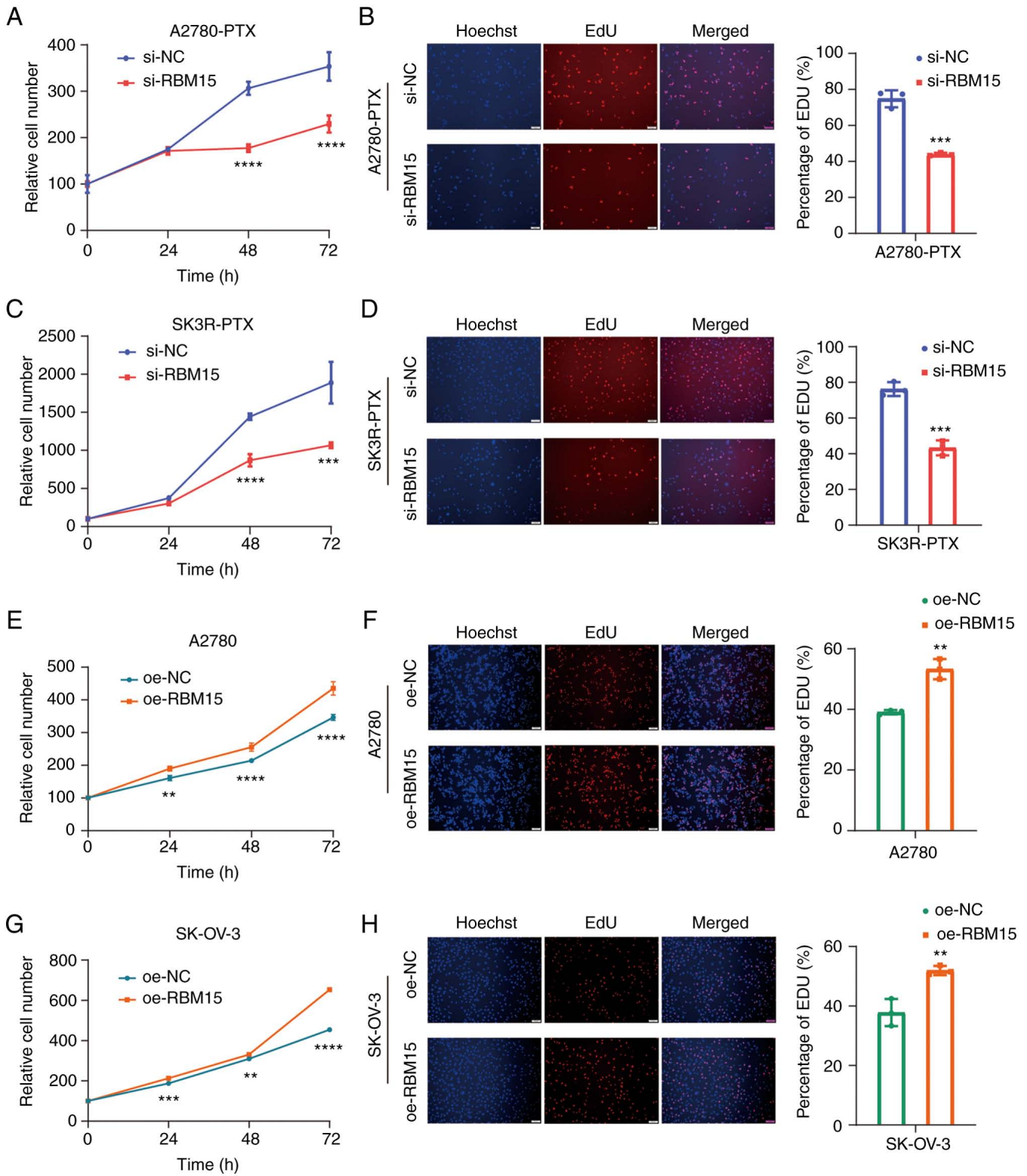


Figure 2. Effect of RBM15 on OC cell proliferation. (A, C, E and G) Detection of cell viability by the CCK-8 assay after RBM15-siRNA (si-RBM15) or RBM15-overexpressing plasmid (oe-RBM15) transfection for 0, 24, 48 and 72 h in A2780-PTX, SK3R-PTX, A2780 and SK-OV-3 cells. Two-way ANOVA followed by the Sidak test was used. Data presented as mean \pm SD (n=3). A2780-PTX: 48 h, $P < 0.0001$; 72 h $P < 0.0001$. SK3R-PTX: 48 h, $P < 0.0001$; 72 h, $P < 0.0001$. A2780: 24 h, $P = 0.0006$, 48 h, $P = 0.0036$; 72 h $P < 0.0001$. SK-OV-3: 24 h, $P = 0.0018$; 48 h, $P < 0.0001$; 72 h, $P < 0.0001$. (B, D, F and H) The EdU assay and statistical analysis following si-RBM15 or oe-RBM15 transfection for 48 h. Original magnification, $\times 100$; Scale bar, 100 μm . All assays were repeated at least three times. An unpaired Student's t-test was used. A2780-PTX, $P = 0.0004$; SK3R-PTX, $P = 0.0006$; A2780, $P = 0.0019$; SK-OV-3, $P = 0.0070$. Data presented as mean \pm SD. ** $P < 0.01$; *** $P < 0.001$; **** $P < 0.0001$. RBM15, RNA binding motif protein 15; OC, ovarian cancer; si, small interfering; oe, overexpressing; NC, negative control; PTX, paclitaxel.

significantly associated with RBM15 expression by correlation test ($P < 0.001$). GO term analysis revealed that these

genes were primarily involved in the Smad protein complex and DNA-binding transcription activator activity

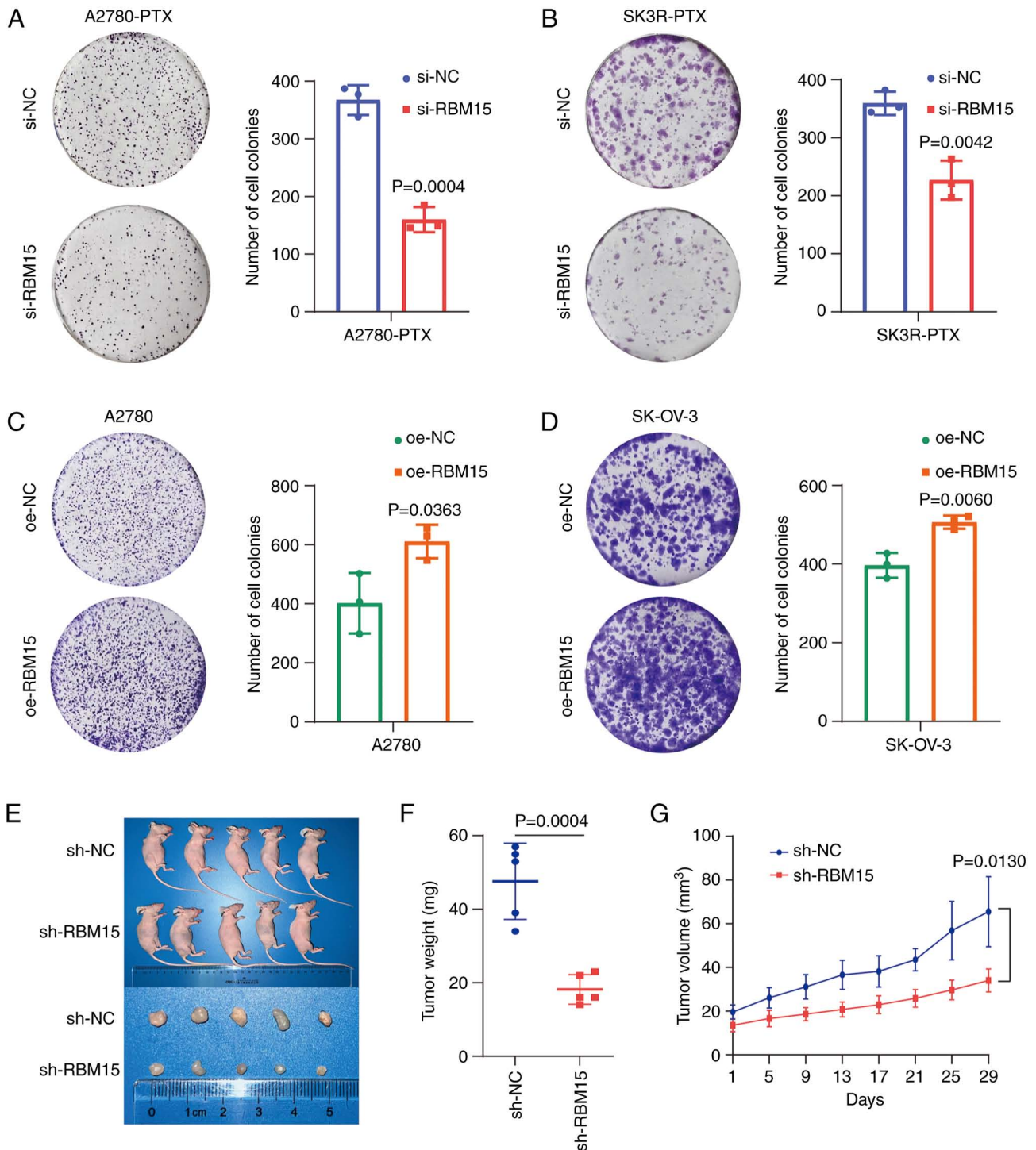


Figure 3. The function of RBM15 on colony formation *in vitro* and tumor growth *in vivo*. (A-D) Detection of colony formation after si-RBM15 and oe-RBM15 transfection for 2 weeks. Histograms show the statistical analyses. Assays were repeated at least three times. An unpaired Student's t-test was used. Data presented as mean \pm SD (n=3). (E) Xenograft tumor formation in nude mice. sh-NC or sh-RBM15-infected A2780-PTX cells were subcutaneously implanted in nude mice (n=5/group). (F) Measurement of tumor weight. An unpaired Student's t-test was used. Data presented as mean \pm SD (n=5). (G) Measurement of tumor size in growth. Two-way ANOVA followed by the Sidak test was used. Data presented as mean \pm SD (n=5). RBM15, RNA binding motif protein 15; si, small interfering; oe, overexpressing; NC, negative control; PTX, paclitaxel; sh, short hairpin.

(Fig. S8A). In addition, KEGG pathway analysis showed that RBM15-correlated (positively or negatively) genes were gathered at the pathways of cellular senescence, RNA degradation, TGF- β signaling and mRNA surveillance (Fig. S8B).

Based on GO and KEGG enrichment analyses, RBM15 expression is related to the TGF- β signaling pathway.

Next, the effect of TGF- β signaling on RBM15 expression was examined. The expression of RBM15 and MDR1 was significantly reduced after TGF- β 1 treatment at the mRNA and protein levels (Fig. 6A-E). The activation of TGF- β 1 was abolished by the addition of the TGF- β receptor inhibitor SB431542. p-Smad2 was markedly low in SK3R-PTX cells compared with SK-OV-3 cells, as detected by western

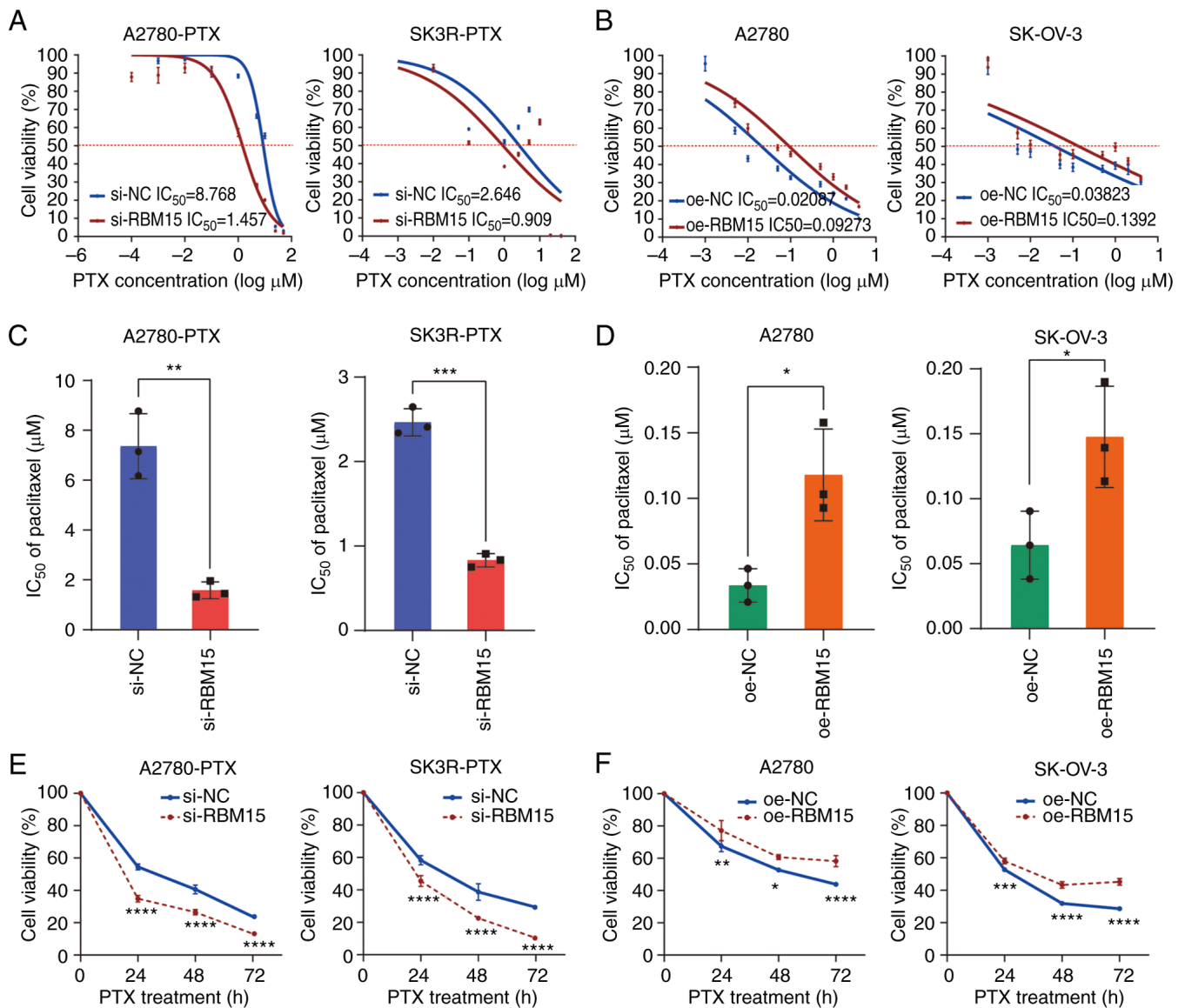


Figure 4. Effect of RBM15 on paclitaxel sensitivity. (A and B) Detection of cell viability by the CCK-8 assays after knockdown or overexpression of RBM15 in A2780-PTX and SK3R-PTX cells treated with different doses of PTX. The IC₅₀ was calculated by nonlinear regression analysis using a model of 'Log(inhibitor) vs. normalized response-Variable slope' under the 'Dose-response-Inhibition' section. Data presented as mean \pm SD (n=4). (C and D) Measurement of IC₅₀ after PTX treatment in siRNA transfected A2780-PTX (P=0.0018) and SK3R-PTX (P<0.0001) cells and overexpressing plasmid transfected A2780 (P=0.0172) and SK-OV-3 (P=0.0371) cells. An unpaired Student's t-test was used. Data presented as mean \pm SD (n=3). (E and F) Detection of cell viability by the CCK-8 assays after knockdown in A2780-PTX and SK3R-PTX cells or overexpression of RBM15 in A2780 and SK-OV-3 cells treated with IC₅₀ dose of PTX for 24, 48 and 72 h. A2780-PTX: 24 h, P<0.0001; 48 h, P<0.0001; 72 h, P<0.0001. SK3R-PTX: 24 h, P<0.0001; 48 h, P<0.0001; 72 h, P<0.0001. A2780: 24 h, P=0.0039; 48 h, P=0.0170; 72 h, P<0.0001. SK-OV-3: 24 h, P=0.0003; 48 h, P<0.0001; 72 h, P<0.0001. Two-way ANOVA followed by the Sidak test was used. Data presented as mean \pm SD. *P<0.05; **P<0.01; ***P<0.001; ****P<0.0001. RBM15, RNA binding motif protein 15; si, small interfering; oe, overexpressing; NC, negative control; PTX, paclitaxel; IC₅₀, half-maximal inhibitory concentration.

blotting (Fig. S9) and was used as an indicator of TGF- β signaling activation. The SBE site was found in the promoter region of RBM15 and the Smad-binding motif is indicated (Fig. 6F). From the JASPAR database, it was predicted that Smad proteins, as transcription factors, could directly bind to the promoter of RBM15. The predicted Smad2 binding sites with different scores in the promoter region-2,000 bp upstream from the TSS of RBM15 are illustrated (Fig. 6G). After constructing two plasmids (P1081 and P780; Fig. 6H), a dual-luciferase reporter gene assay was performed. The results showed that the relative luciferase activity was significantly decreased in 293T cells transfected with the

P1081 plasmid, but not with the P780 plasmid, in the presence of 10 ng/ml TGF- β 1 (Fig. 6I). These data indicated that TGF- β 1 affects RBM15 expression through direct Smad-binding events.

Discussion

The present study demonstrated that RBM15 was upregulated in OC tissues and PTX-resistant cells and was associated with poor prognosis in OC patients. Overexpression of RBM15 modulated cell proliferation, chemoresistance and cancer cell stemness, whereas knockdown RBM15 reduced colony

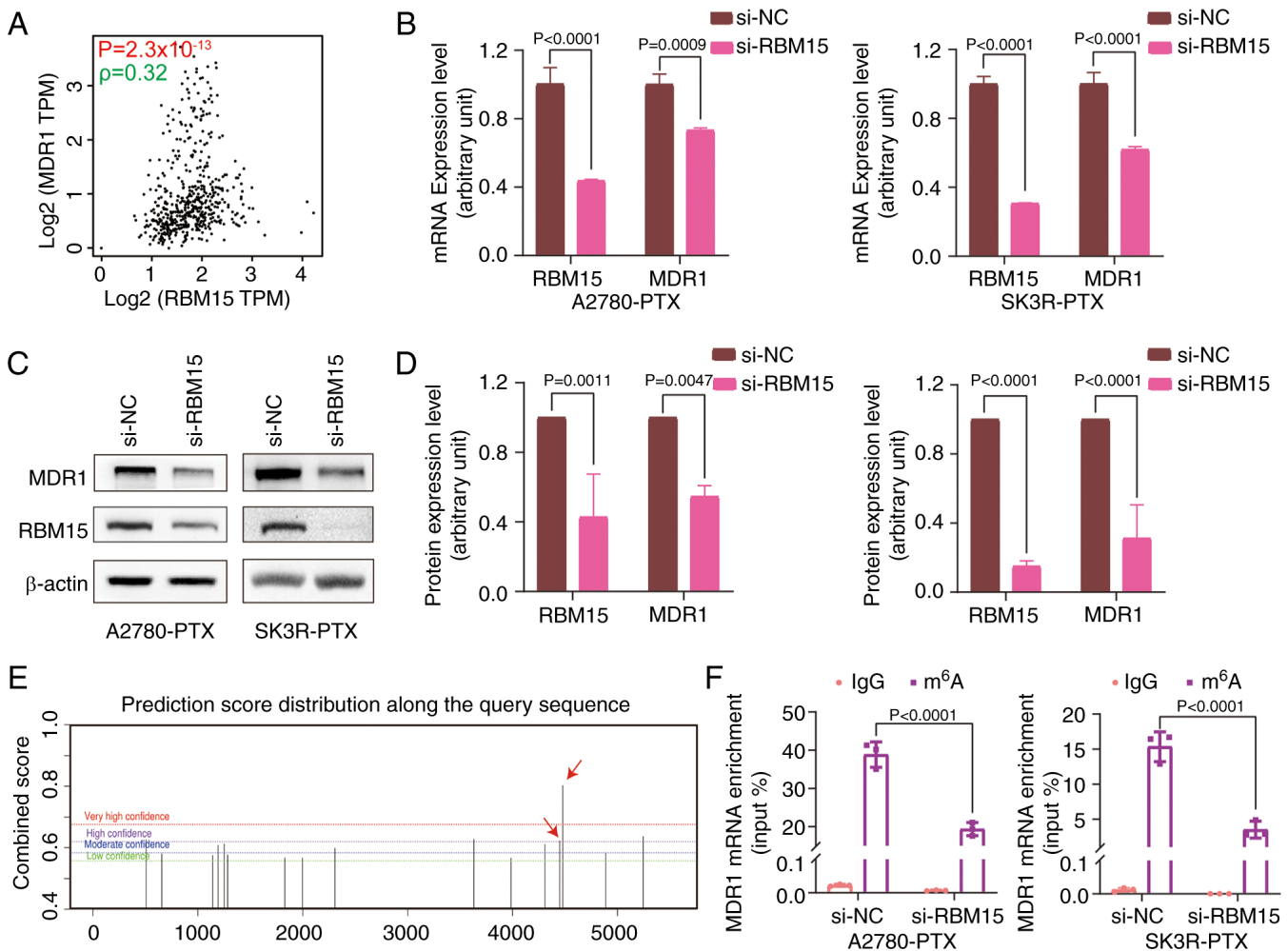


Figure 5. Regulation of MDR1 expression and mRNA m⁶A modification by RBM15. (A) Correlation analysis (Spearman Correlation Coefficient) between expression levels of MDR1 and RBM15. Detection of MDR1 and RBM15 expression at mRNA and protein levels by (B) RT-qPCR and (C) western blotting after si-NC or si-RBM15 transfection in A2780-PTX and SK3R-PTX cells. (D) Semiquantitative analysis of blots in (C). Two-way ANOVA followed by the Sidak test was used. Data presented as mean \pm SD (n=3). (E) Prediction of the distribution of MDR1 mRNA m⁶A methylation sites by the SRAMP database. The red arrow indicates two m⁶A sites (4449 and 4478). (F) MeRIP and RT-qPCR analysis of m⁶A levels in MDR1 mRNA in A2780-PTX and SK3R-PTX cell lines. The well-designed primers for amplifying the fragment covered two adjacent sites (4449 and 4478) were used and MDR1 mRNA was detected by RT-qPCR. Two-way ANOVA followed by the Tukey test was used. Data presented as mean \pm SD (n=3). MDR1, multidrug resistance 1; RBM15, RNA binding motif protein 15; si, small interfering; NC, negative control; PTX, paclitaxel; RT-qPCR, reverse transcription-quantitative PCR; MeRIP, methylated RNA immunoprecipitation.

formation *in vitro* and tumor formation *in vivo*. Furthermore, TGF- β /Smad directly regulated RBM15, which methylates MDR1 mRNA in an m⁶A-dependant manner to mediate chemoresistance.

It has been reported that RBM15 is capable of facilitating cell proliferation in some cancers (16,17,35), but this has not been reported in OC. For example, RBM15 enhances the proliferation, migration and invasion of clear cell renal cell carcinoma (36). The knockdown of RBM15 reduces the proliferation of laryngeal squamous cell cancer both *in vitro* and *in vivo* (16). The current study demonstrated the oncogenic role of RBM15: Overexpression accelerated cell proliferation and colony formation *in vitro* and knockdown of RBM15 suppressed tumor formation *in vivo*. Furthermore, the involvement of RBM15 in PTX resistance in OC was reported.

CSCs, the main culprit of cancer resistance, are a subgroup of bulk tumors with stem cell-like properties and tumorigenic abilities (37,38). The current study observed

that PTX-resistant cells had spheroid-forming capabilities, suggesting the existence of a stem cell-like cell subpopulation. To date, CSC subpopulations have been identified in malignant ovarian tumors, ascites and cancer cell lines by several groups, including ours (7,8,39). It has been reported that CSCs are involved in the development of metastasis, recurrence and drug resistance of OC (40). CSC marker CD44 can upregulate MDR1 expression, leading to increasing the resistance of osteosarcoma cells to doxorubicin (10). Notably, direct regulation of MDR1 expression by RBM15 was observed. Silencing of RBM15 resensitized OC cells to PTX by decreasing MDR1 expression. Using the SRAMP database to predict the possible distribution of m⁶A sites in MDR1 mRNA, the present study explored, for the first time to the best of the authors' knowledge, that RBM15 mediated MDR1 expression through mRNA m⁶A methylation. It has been shown that RBM15 acts as an m⁶A writer to reduce target RNA m⁶A modifications (41,42), ultimately reducing target expression. MDR1 is the best-characterized transporter

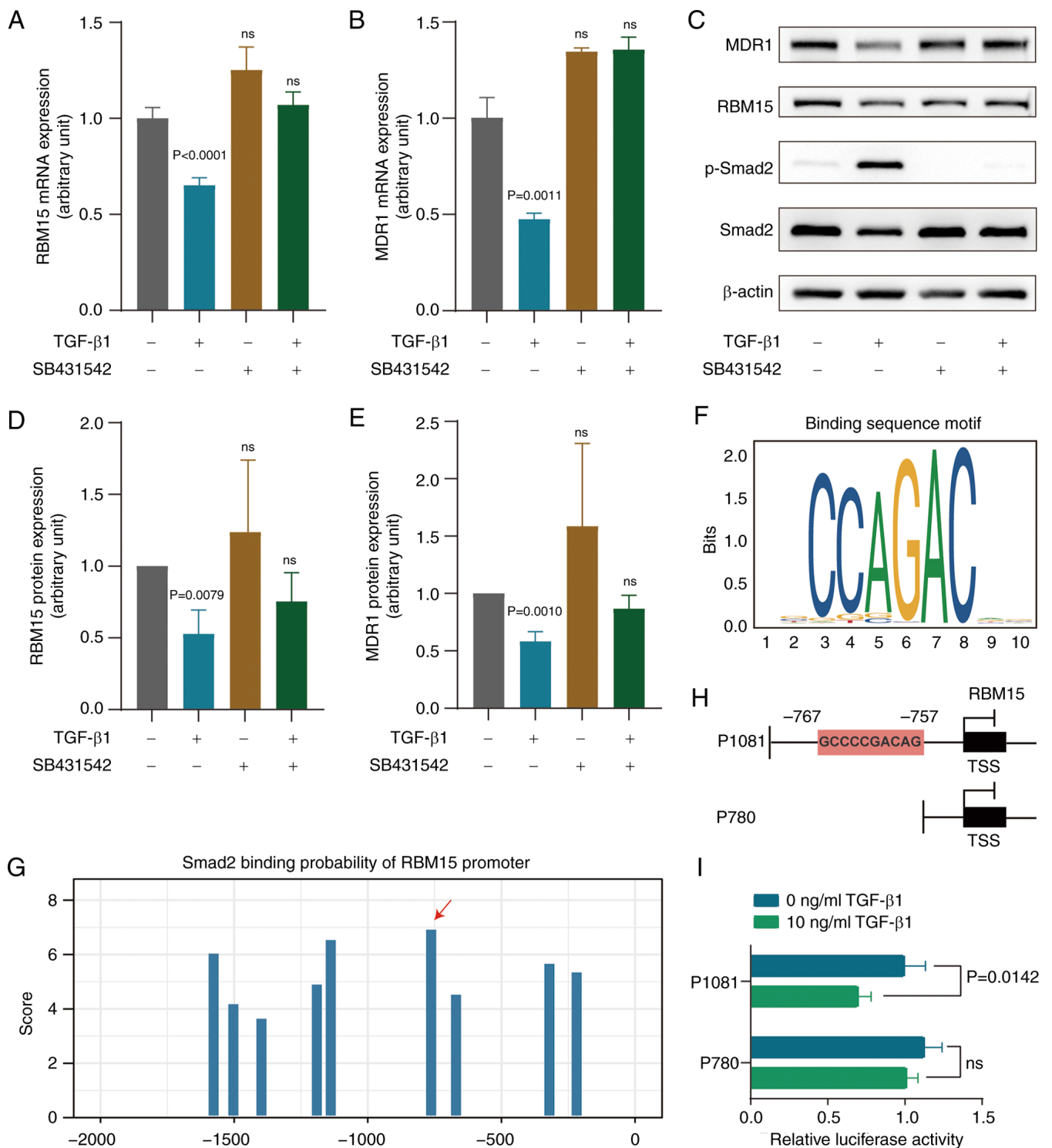


Figure 6. Effect of TGF- β 1 on RBM15 and expression. (A and B) Detection of RBM15 and MDR1 mRNA expression by RT-qPCR after TGF- β 1 (10 ng/ml) treatment in the presence or absence of SB431542 (10 mM) in SK3R-PTX cells. Multiple t-tests were used for multiple groups comparison. Data presented as mean \pm SD (n=3). (C) Detection of MDR1, RBM15, phosphor-Smad2 and Smad2 proteins by western blotting after TGF- β 1 (10 ng/ml) treatment in the presence or absence of SB431542 (10 mM) in SK3R-PTX cells. (D and E) Semiquantitative of membranes in C. Multiple t-tests were used for multiple groups comparison. Data presented as mean \pm SD (n=3). (F) The Smad binding motif. (G) The binding sites of Smad2 in the region -2,000 bp upstream of the RBM15 TSS were predicted from the JASPAR database. (H) Schematic illustrations of two RBM15 plasmid constructs (P1081 and P780): -1,081 bp and -780 bp upstream from TSS in the RBM15 promoter region. (I) Luciferase activities were detected in 293T cells transfected with different RBM15 promoter-reporter plasmids in the presence or absence of TGF- β 1 (10 ng/ml). Two-way ANOVA followed by the Sidak test was used. Data presented as mean \pm SD (n=3). ns, not significant (P>0.05). RBM15, RNA binding motif protein 15; MDR1, multidrug resistance 1; RT-qPCR, reverse transcription-quantitative PCR; PTX, paclitaxel; TSS, transcriptional start site; p-, phosphorylated.

protein whose overexpression can confer resistance to cytotoxic and targeted chemotherapy (43). A number of studies

have shown that MDR1 is a primary target for reversing drug resistance in OC (44-46) and m⁶A modification of

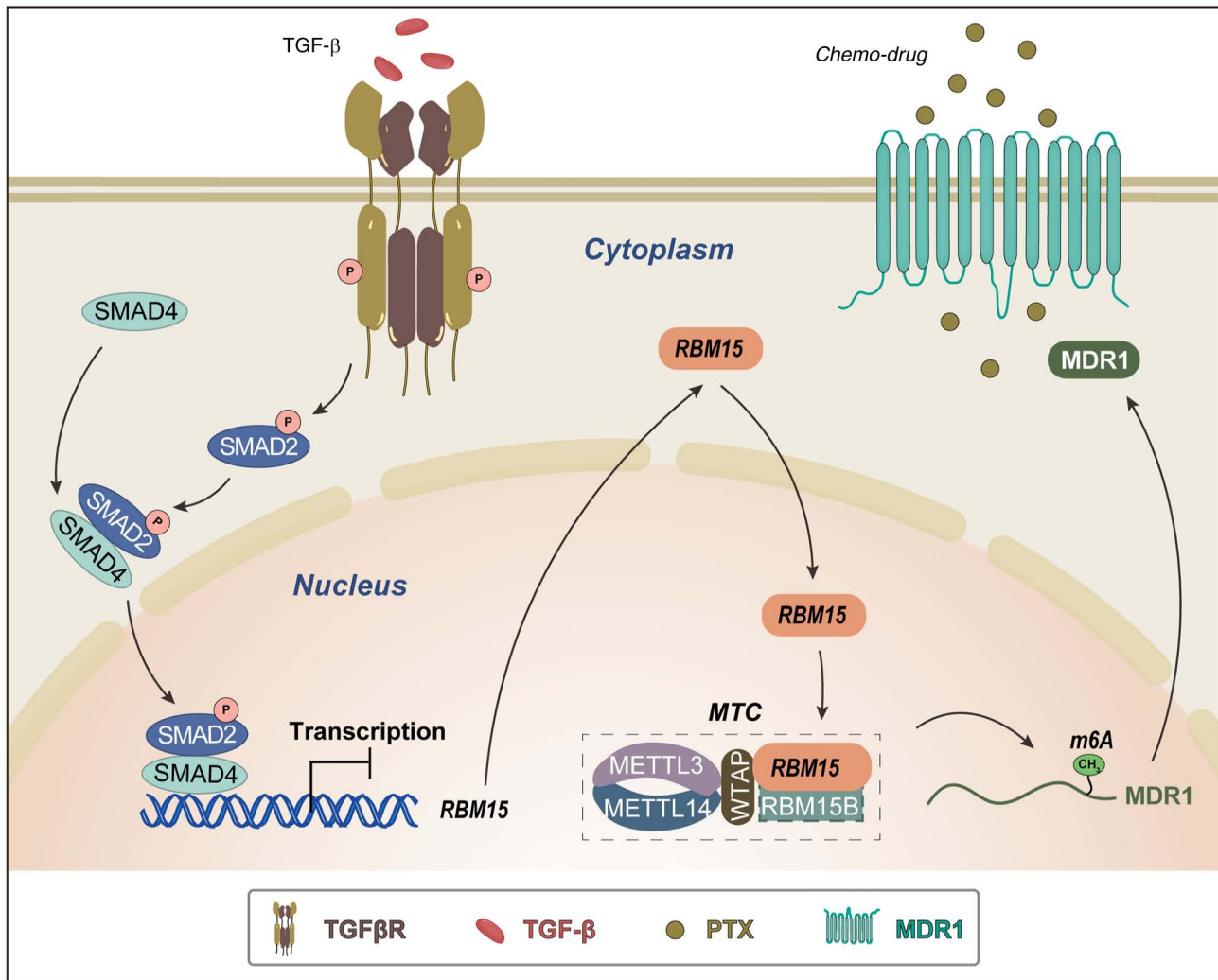


Figure 7. The schematic model illustrates the regulatory mechanism of RBM15 in PTX-resistant ovarian cancer cells. RBM15, RNA binding motif protein 15; MDR1, multidrug resistance 1; METTL, methyltransferase-like protein; MTC, methyltransferase complex; PTX, paclitaxel; Smad, similar to Sma from *Caenorhabditis elegans* and Mad (mothers against decapentaplegic) from *Drosophila*; TGFβR, TGF-β receptor; WTAP, Wilms tumor 1-associated protein.

RNA primarily affects RNA processing, degradation and translation to regulate gene expression, tumorigenesis and progression (47). The findings of the present study supported the role of RBM15 in the regulation of MDR1 expression, at least through m⁶A modifications.

The present study also examined the upstream regulation of RBM15 via the TGF-β signaling pathway. TGF-β is a cytokine closely involved in a number of cancer cell processes, including cell death, proliferation, metastasis, mesenchymal-epithelial transition, cancer cell stemness and chemoresistance (48,49). Our previous study found that the TGF-β signaling pathway was deficient in PTX-resistant OC cells (21). The present study observed that enhancement of TGF-β signaling led to the downregulation of RBM15 expression at the mRNA and protein levels in PTX-resistant OC cells by directly binding to the RBM15 promoter through the SBE site. These data indicated that the TGF-β/RBM15/MDR1 axis is involved in the development of chemoresistance in OC cells.

In conclusion, RBM15 was upregulated in OC tissues and PTX-resistant cells. High expression of RBM15 was associated

with poor prognosis in OC patients. Silencing of RBM15 down-regulated the expression MDR1 by decreasing MDR1 mRNA m⁶A methylation. The TGF-β signaling pathway activates and phosphorylates Smad2, which directly binds to RBM15 on its promoter, thereby suppressing RBM15 expression. These findings revealed RBM15 as a tissue biomarker for OC and PTX resistance and a TGF-β/RBM15/MDR1 regulatory mechanism. Targeting RBM15 may provide a novel therapeutic strategy for the treatment of PTX-resistant OC (Fig. 7).

Acknowledgments

The authors thank Dr Jiming Shi (Jinshan Hospital of Fudan University) for the pathological evaluation.

Funding

The present study was supported by grants from the National Natural Science Foundation of China (grant no. 81872121) and the Science and Technology Commission of Shanghai Municipality (grant no. 23ZR1408900) to GX.

Availability of data and materials

The datasets used and/or analyzed during the current study are available from the corresponding author on reasonable request.

Authors' contributions

JY contributed to experimental performance, data analyses, figure preparation and manuscript drafts. WG contributed to the design of the siRNA and qPCR primers and data analysis. XL, FW and HL contributed to the cell culture, bioinformatics analysis and validation. GX contributed to the supervision, conceptualization and project administration and wrote and edited the final manuscript. JY, WG and GX confirm the authenticity of all the raw data. All authors contributed to the manuscript and approved the final version.

Ethics approval and consent to participate

The ethical approval for human subjects was approved by the Ethics Committee of Jinshan Hospital (approval no. JYLLKY-2019-01-01) and was approved by the Ethics Committee of the Shanghai Outdo Biotech Company (approval no. TRLL-2020-035-01). Animal studies were approved by the Laboratory Animal Welfare and Ethics Committee of the Shanghai Public Health Clinical Center (approval no. GWLL2020-A0270-01).

Patient consent for publication

Not applicable.

Competing interests

The authors declare that they have no competing interests.

Authors' information

Professor Guoxiong Xu ORCID: 0000-0002-9074-8754.

References

- Siegel RL, Miller KD, Fuchs HE and Jemal A: Cancer statistics, 2022. *CA Cancer J Clin* 72: 7-33, 2022.
- Lheureux S, Braunstein M and Oza AM: Epithelial ovarian cancer: Evolution of management in the era of precision medicine. *CA Cancer J Clin* 69: 280-304, 2019.
- Lheureux S, Gourley C, Vergote I and Oza AM: Epithelial ovarian cancer. *Lancet* 393: 1240-1253, 2019.
- Ramos A, Sadeghi S and Tabatabaieian H: Battling chemoresistance in cancer: Root causes and strategies to uproot them. *Int J Mol Sci* 22: 9451, 2021.
- Hrycyna CA: Molecular genetic analysis and biochemical characterization of mammalian P-glycoproteins involved in multidrug resistance. *Semin Cell Dev Biol* 12: 247-256, 2001.
- Ahmed N, Escalona R, Leung D, Chan E and Kannourakis G: Tumour microenvironment and metabolic plasticity in cancer and cancer stem cells: Perspectives on metabolic and immune regulatory signatures in chemoresistant ovarian cancer stem cells. *Semin Cancer Biol* 53: 265-281, 2018.
- Wang F, Zhang L, Liu J, Zhang J and Xu G: Highly expressed STAT1 contributes to the suppression of stemness properties in human paclitaxel-resistant ovarian cancer cells. *Aging (Albany NY)* 12: 11042-11060, 2020.
- Foster R, Buckanovich RJ and Rueda BR: Ovarian cancer stem cells: Working towards the root of stemness. *Cancer Lett* 338: 147-157, 2013.
- Garson K and Vanderhyden BC: Epithelial ovarian cancer stem cells: Underlying complexity of a simple paradigm. *Reproduction* 149: R59-R70, 2015.
- Gerardo-Ramirez M, Keggenhoff FL, Giam V, Becker D, Groth M, Hartmann N, Straub BK, Morrison H, Galle PR, Marquardt JU, *et al*: CD44 contributes to the regulation of MDR1 protein and doxorubicin chemoresistance in osteosarcoma. *Int J Mol Sci* 23: 8616, 2022.
- Zaccara S, Ries RJ and Jaffrey SR: Reading, writing and erasing mRNA methylation. *Nat Rev Mol Cell Biol* 20: 608-624, 2019.
- Lan Q, Liu PY, Bell JL, Wang JY, Hüttelmaier S, Zhang XD, Zhang L and Liu T: The emerging roles of RNA m⁶A methylation and demethylation as critical regulators of tumorigenesis, drug sensitivity, and resistance. *Cancer Res* 81: 3431-3440, 2021.
- Hiriart E, Gruffat H, Buisson M, Mikaelian I, Keppler S, Meresse P, Mercher T, Bernard OA, Sergeant A and Manet E: Interaction of the Epstein-Barr virus mRNA export factor EB2 with human Spen proteins SHARP, OTT1, and a novel member of the family, OTT3, links Spen proteins with splicing regulation and mRNA export. *J Biol Chem* 280: 36935-36945, 2005.
- Yang Y, Hsu PJ, Chen YS and Yang YG: Dynamic transcriptomic m⁶A decoration: writers, erasers, readers and functions in RNA metabolism. *Cell Res* 28: 616-624, 2018.
- Yang F, Liu Y, Xiao J, Li B, Chen Y, Hu A, Zeng J, Liu Z and Liu H: Circ-CTNNB1 drives aerobic glycolysis and osteosarcoma progression via m⁶A modification through interacting with RBM15. *Cell Prolif* 56: e13344, 2023.
- Wang X, Tian L, Li Y, Wang J, Yan B, Yang L, Li Q, Zhao R, Liu M, Wang P and Sun Y: RBM15 facilitates laryngeal squamous cell carcinoma progression by regulating TMBIM6 stability through IGF2BP3 dependent. *J Exp Clin Cancer Res* 40: 80, 2021.
- Zhao Z, Ju Q, Ji J, Li Y and Zhao Y: N⁶-methyladenosine methylation regulator RBM15 is a potential prognostic biomarker and promotes cell proliferation in pancreatic adenocarcinoma. *Front Mol Biosci* 9: 842833, 2022.
- Wang H, Zhao X and Lu Z: m⁶A RNA methylation regulators act as potential prognostic biomarkers in lung adenocarcinoma. *Front Genet* 12: 622233, 2021.
- Jang KH, Heras CR and Lee G: m⁶A in the signal transduction network. *Mol Cells* 45: 435-443, 2022.
- Kwok AL, Wong OG, Wong ES, Tsun OK, Chan KK and Cheung AN: Caution over use of ES2 as a model of ovarian clear cell carcinoma. *J Clin Pathol* 67: 921-922, 2014.
- Zhang J, Guan W, Xu X, Wang F, Li X and Xu G: A novel homeostatic loop of sorcin drives paclitaxel-resistance and malignant progression via Smad4/ZEB1/miR-142-5p in human ovarian cancer. *Oncogene* 40: 4906-4918, 2021.
- Livak KJ and Schmittgen TD: Analysis of relative gene expression data using real-time quantitative PCR and the 2(-Delta Delta C(T)) method. *Methods* 25: 402-408, 2001.
- Zhang L, Zhou D, Guan W, Ren W, Sun W, Shi J, Lin Q, Zhang J, Qiao T, Ye Y, *et al*: Pyridoxine 5'-phosphate oxidase is a novel therapeutic target and regulated by the TGF- β signalling pathway in epithelial ovarian cancer. *Cell Death Dis* 8: 3214, 2017.
- Edgar R, Domrachev M and Lash AE: Gene expression omnibus: NCBI gene expression and hybridization array data repository. *Nucleic Acids Res* 30: 207-210, 2002.
- Ritchie ME, Phipson B, Wu D, Hu Y, Law CW, Shi W and Smyth GK: limma powers differential expression analyses for RNA-seq and microarray studies. *Nucleic Acids Res* 43: e47, 2015.
- Chandrashekar DS, Bashel B, Balasubramanya SAH, Creighton CJ, Ponce-Rodriguez I, Chakravarthi BVSK and Varambally S: UALCAN: A portal for facilitating tumor subgroup gene expression and survival analyses. *Neoplasia* 19: 649-658, 2017.
- Yu G, Wang LG, Han Y and He QY: clusterProfiler: An R package for comparing biological themes among gene clusters. *OMICS* 16: 284-287, 2012.
- Gyorffy B, Lánczky A and Szállási Z: Implementing an online tool for genome-wide validation of survival-associated biomarkers in ovarian-cancer using microarray data from 1287 patients. *Endocr Relat Cancer* 19: 197-208, 2012.
- Tang Z, Li C, Kang B, Gao G, Li C and Zhang Z: GEPIA: A web server for cancer and normal gene expression profiling and interactive analyses. *Nucleic Acids Res* 45 (W1): W98-W102, 2017.

30. Geeleher P, Cox N and Huang RS: pRRophetic: An R package for prediction of clinical chemotherapeutic response from tumor gene expression levels. *PLoS One* 9: e107468, 2014.
31. Zhou Y, Zeng P, Li YH, Zhang Z and Cui Q: SRAMP: Prediction of mammalian N6-methyladenosine (m6A) sites based on sequence-derived features. *Nucleic Acids Res* 44: e91, 2016.
32. Castro-Mondragon JA, Riudavets-Puig R, Rauluseviciute I, Lemma RB, Turchi L, Blanc-Mathieu R, Lucas J, Boddie P, Khan A, Manosalva Pérez N, *et al*: JASPAR 2022: The 9th release of the open-access database of transcription factor binding profiles. *Nucleic Acids Res* 50 (D1): D165-D173, 2022.
33. Bowen NJ, Walker LD, Matyunina LV, Logani S, Totten KA, Benigno BB and McDonald JF: Gene expression profiling supports the hypothesis that human ovarian surface epithelia are multipotent and capable of serving as ovarian cancer initiating cells. *BMC Med Genomics* 2: 71, 2009.
34. Yoshihara K, Tajima A, Komata D, Yamamoto T, Kodama S, Fujiwara H, Suzuki M, Onishi Y, Hatae M, Sueyoshi K, *et al*: Gene expression profiling of advanced-stage serous ovarian cancers distinguishes novel subclasses and implicates ZEB2 in tumor progression and prognosis. *Cancer Sci* 100: 1421-1428, 2009.
35. Dong H, Zhang H, Mao X, Liu S, Xu W and Zhang Y: RBM15 promotes the proliferation, migration and invasion of pancreatic cancer cell lines. *Cancers (Basel)* 15: 1084, 2023.
36. Zeng X, Chen K, Li L, Tian J, Ruan W, Hu Z, Peng D and Chen Z: Epigenetic activation of RBM15 promotes clear cell renal cell carcinoma growth, metastasis and macrophage infiltration by regulating the m6A modification of CXCL11. *Free Radic Biol Med* 184: 135-147, 2022.
37. Ayob AZ and Ramasamy TS: Cancer stem cells as key drivers of tumour progression. *J Biomed Sci* 25: 20, 2018.
38. Abdullah LN and Chow EKH: Mechanisms of chemoresistance in cancer stem cells. *Clin Transl Med* 2: 3, 2013.
39. Elzarkaa AA, Sabaa BE, Abdelkhalik D, Mansour H, Melis M, Shaalan W, Farouk M, Malik E and Soliman AA: Clinical relevance of CD44 surface expression in advanced stage serous epithelial ovarian cancer: A prospective study. *J Cancer Res Clin Oncol* 142: 949-958, 2016.
40. Gao Y, Foster R, Yang X, Feng Y, Shen JK, Mankin HJ, Hornicek FJ, Amiji MM and Duan Z: Up-regulation of CD44 in the development of metastasis, recurrence and drug resistance of ovarian cancer. *Oncotarget* 6: 9313-9326, 2015.
41. Cai X, Chen Y, Man D, Yang B, Feng X, Zhang D, Chen J and Wu J: RBM15 promotes hepatocellular carcinoma progression by regulating N6-methyladenosine modification of YES1 mRNA in an IGF2BP1-dependent manner. *Cell Death Discov* 7: 315, 2021.
42. Fang J, Wu X, He J, Zhang H, Chen X, Zhang H, Novakovic B, Qi H and Yu X: RBM15 suppresses hepatic insulin sensitivity of offspring of gestational diabetes mellitus mice via m6A-mediated regulation of CLDN4. *Mol Med* 29: 23, 2023.
43. Takara K, Sakaeda T and Okumura K: An update on overcoming MDR1-mediated multidrug resistance in cancer chemotherapy. *Curr Pharm Des* 12: 273-286, 2006.
44. Huang W, Yang S, Cheng YS, Sima N, Sun W, Shen M, Braisted JC, Lu W and Zheng W: Terfenadine resensitizes doxorubicin activity in drug-resistant ovarian cancer cells via an inhibition of CaMKII/CREB1 mediated ABCB1 expression. *Front Oncol* 12: 1068443, 2022.
45. Su S, Sun X, Zhang Q, Zhang Z and Chen J: CCL20 promotes ovarian cancer chemotherapy resistance by regulating ABCB1 expression. *Cell Struct Funct* 44: 21-28, 2019.
46. Vaidyanathan A, Sawers L, Gannon AL, Chakravarty P, Scott AL, Bray SE, Ferguson MJ and Smith G: ABCB1 (MDR1) induction defines a common resistance mechanism in paclitaxel- and olaparib-resistant ovarian cancer cells. *Br J Cancer* 115: 431-441, 2016.
47. Wang T, Kong S, Tao M and Ju S: The potential role of RNA N6-methyladenosine in Cancer progression. *Mol Cancer* 19: 88, 2020.
48. Ikushima H and Miyazono K: TGFbeta signalling: A complex web in cancer progression. *Nat Rev Cancer* 10: 415-424, 2010.
49. Katsuno Y, Meyer DS, Zhang Z, Shokat KM, Akhurst RJ, Miyazono K and Derynck R: Chronic TGF-β exposure drives stabilized EMT, tumor stemness, and cancer drug resistance with vulnerability to bitopic mTOR inhibition. *Sci Signal* 12: eaau8544, 2019.



Copyright © 2023 Yuan et al. This work is licensed under a Creative Commons Attribution-NonCommercial-NoDerivatives 4.0 International (CC BY-NC-ND 4.0) License.